

# Toward the Design of Mutation-Resistant Enzyme Inhibitors: Further Evaluation of the Substrate Envelope Hypothesis

Visvaldas Kairys<sup>1</sup>, Michael K. Gilson<sup>2</sup>,  
Viney Lather<sup>1</sup>, Celia A. Schiffer<sup>3</sup> and  
Miguel X. Fernandes<sup>1,\*</sup>

<sup>1</sup>Centro de Química da Madeira, Departamento de Química, Universidade da Madeira, Campus da Penteada, 9000-390 Funchal, Portugal

<sup>2</sup>Center for Advanced Research in Biotechnology, University of Maryland Biotechnology Institute, 9600 Gudelsky Drive, Rockville, MD 20850, USA

<sup>3</sup>Department of Biochemistry and Molecular Pharmacology, University of Massachusetts Medical School, 364 Plantation Street, Worcester, MA 01605-2324, USA

\*Corresponding author: Miguel X. Fernandes, mxf@uma.pt

**Previous studies have shown the usefulness of the substrate envelope concept in the analysis and prediction of drug resistance profiles for human immunodeficiency virus protease mutants. This study tests its applicability to several other therapeutic targets: Abl kinase, chitinase, thymidylate synthase, dihydrofolate reductase, and neuraminidase. For the targets where many ( $\geq 6$ ) mutation data are available to compute the average mutation sensitivity of inhibitors, the total volume of an inhibitor molecule that projects outside the substrate envelope  $V_{out}$ , is found to correlate with average mutation sensitivity. Analysis of a locally computed volume suggests that the same correlation would hold for the other targets, if more extensive mutation data sets were available. It is concluded that the substrate envelope concept offers a promising and easily implemented computational tool for the design of drugs that will tend to resist mutations. Software implementing these calculations is provided with the 'Supporting Information'.**

**Key words:** mutation resistance, substrate envelope

**Abbreviations:** CHARMM, Chemistry at Harvard Molecular Mechanics; DHFR, dihydrofolate reductase; FP2/FP3, Tanimoto coefficient based on daylight/hexadecimal type fingerprints; HIV, human immunodeficiency virus;  $IC_{50}$ , concentration to achieve 50% of inhibition; M.W., molecular weight;  $N_{heavy}$ , number of non-hydrogen atoms; RMSD, root mean square deviation;  $V_{in}$ , volume of the inhibitor inside of the substrate envelope;  $V_{out}$ , volume of the inhibitor outside of the substrate envelope;  $V_{out,loc}$ , volume of inhibitor outside of substrate envelope and local to mutated residues.

Received 7 April 2009, revised 26 June 2009 and accepted for publication 28 June 2009

Drug resistance is a serious challenge in the treatment of many diseases, leading to morbidity, mortality, and medical costs (1–3). Resistance typically emerges when a population of pathogens or cancer cells is subjected to selection pressure in the course of treatment with a drug. Under these conditions, resistant variants can come to dominate the cellular population, making the drug ineffective. A number of mechanisms can lead to drug resistance, including decreased transport of drug to its site of action, increased elimination from the site of action, metabolic inactivation of the drug, ineffective activation of a prodrug, upregulation of alternative pathways, overexpression of the targeted protein, and mutation of the target to reduce its affinity for the drug (4). Ideally, such mechanisms would be accounted for in the course of drug discovery to prevent the emergence of resistance at the outset, rather than having to address it after it appears. The present study explores a method of designing drugs that will be robust in the face of mutations in a targeted enzyme.

Adaptive inhibitors (5), which contain rotatable bonds that can position several alternative functionalities at variable regions of the binding site, offer one important strategy for the design of mutation-resistant inhibitors. Such compounds may retain affinity when the target protein mutates, because they can adapt conformationally, apposing their most complementary moieties to the mutated residue. The present study elaborates a different approach, the design of enzyme inhibitors that fit within the known 'substrate envelope' of the targeted enzyme (6).

According to the substrate envelope hypothesis, inhibitors fitting within the three-dimensional region occupied by the enzyme's natural substrate should tend to resist mutations, because mutations that could knock out inhibitor binding would also knock out substrate binding, rendering the enzyme ineffective. This idea was first advanced in the context of human immunodeficiency virus (HIV), which cleaves the Gag-Pol polyprotein at sites with a number of different amino acid sequences (7). Chellappan *et al.* retrospectively evaluated the substrate envelope hypothesis for HIV protease by computing the volumes of clinically approved HIV-1 protease inhibitors lying outside the substrate envelope ( $V_{out}$ ) (8), and comparing these volumes with the mutation resistance profiles of the respective inhibitors. They found that the values of  $V_{out}$  correlated with

the sensitivity of the inhibitors to clinically relevant mutations, although the correlation was somewhat dependent on the mutation set chosen. In a second study, Chellappan *et al.* furthermore used  $V_{\text{out}}$  prospectively, as part of a scoring function for the computational design of a compound library targeting HIV protease, and observed that the compounds with the smallest values of  $V_{\text{out}}$  were most robust to clinically relevant protease mutations (9). Thus, although the substrate envelope hypothesis is based upon a somewhat simplistic steric model, early studies suggest that it may be a useful guide to the design of mutation-resistant drugs. More recently, Altman *et al.* applied inverse design using substrate envelope to develop mutation robust subnanomolar inhibitors of HIV protease (10).

It is now interesting to consider whether the substrate envelope hypothesis is applicable to other drug targets, as recently suggested (11). Encouragingly, Colman and co-workers (12–14) have observed that those inhibitors of flu virus neuraminidase, which are most similar to the transition state of the enzyme's natural substrate, are the most mutation-resistant, although they did not suggest a quantifying measure of this relationship. This paper describes a retrospective study of the applicability of a quantitative form of the substrate envelope concept, suitable for use in structure-based drug design, to a series of additional enzymes regarded as drug targets.

## Methods

### Concepts and approach

The central question to be addressed is whether the volume of an inhibitor falling outside the region of the active site occupied by bound substrate correlates with the tendency of the inhibitor to lose affinity in the face of mutations that do not destroy enzyme activity. Answering this question retrospectively requires affinity data for multiple inhibitors with wild type and mutant enzyme, along with three-dimensional structural data. An ideal data set would include mutations in many parts of the active site, so that any extension of the inhibitor outside the substrate envelope would be probed by at least one mutation. In this case, the total volume of inhibitor outside the substrate envelope,  $V_{\text{out}}$  (see 'Calculation of inhibitor volumes outside substrate envelope'), might be expected to correlate with the average, over all mutants, of the loss of affinity, expressed for each mutant  $i$  as the sensitivity  $s_i = \log\left(\frac{K_{\text{mut},i}}{K_{\text{wt}}}\right)$ . Here  $K_{\text{mut},i}$  and  $K_{\text{wt}}$  are, respectively, the dissociation constants or  $\text{IC}_{50}$  values of the inhibitor with mutant  $i$  and the wild type, and the logarithm generates a quantity proportional to the difference in binding free energy. When a large set of mutation data are available, the average of  $s_i$  over the mutants  $i$  quantifies the overall sensitivity of the inhibitor to mutations.

When less comprehensive mutation data are available, an extension of the ligand outside the substrate envelope may not be probed by any of the available mutations, so loss of affinity may fail to correlate with  $V_{\text{out}}$ . However, such an instance does not necessarily invalidate the substrate envelope hypothesis, because, in the clinical setting, it is likely that the targeted cell population will in fact generate mutations that probe other parts of the active site. In this

case, the full degree to which the ligand extends outside the substrate envelope may indeed become important. For less comprehensive mutation sets, it is still of interest to determine whether the volume of an inhibitor outside the substrate envelope *in the vicinity of the mutated residues* in the available data set, here termed  $V_{\text{out,loc}}$  (see 'Calculation of inhibitor volumes outside substrate envelope'), correlates with sensitivity to those mutations. Such a result would tend to support the general idea that the most mutation-resistant inhibitors are those which fall entirely within the substrate envelope.

### Experimental data

For each enzyme to be analyzed, the present study employs crystal structures with substrate and the inhibitors of interest, along with the measured affinities of the inhibitors for the wild-type enzyme and a collection of mutants. Table 1 lists the enzymes, substrates, and inhibitors studied here, along with the Protein Data Bank (PDB) IDs (15) of the crystal structures employed. Table 2 shows the mutations considered, the inhibitors, and the nature of the affinity data ( $K_d$ ,  $K_i$ , or  $\text{IC}_{50}$ ). The mutation sensitivities for each inhibitor used in this paper are listed in Table S1. Most of the affinity data were drawn from BindingDB (16). The investigated mutations arose *in vivo* as a response to a drug, or were produced in the course of directed mutagenesis studies aimed at discovering resistance mutations of the inhibitors.

As shown in Table 2, all 4 Abl kinase inhibitors have been tested experimentally against the same set of 8 mutant enzymes, all 3 chitinase inhibitors have been tested against the same set of 6 mutants, and both thymidylate synthase (TS) inhibitors have been tested against the same 11 mutants. However, two of the four inhibitors of dihydrofolate reductase (DHFR) have been tested against two mutants, and the other two inhibitors have been tested against a different mutant. For the sake of consistency, the two pairs of inhibitors are analyzed separately, each with respect to its own set of mutant data. Similarly, two separate analyses are done for the neuraminidase inhibitors, one for the inhibitors tested only against R292K, the other for the inhibitors tested against the larger set of six mutants, as listed in Table 2.

### Calculation of inhibitor volumes outside substrate envelope

The volume of an inhibitor outside the substrate envelope,  $V_{\text{out}}$ , was computed much as done previously (8). One difference is that the prior studies of HIV protease constructed a model of the substrate envelope from multiple crystal structures, each with a different substrate bound, but here, there is only a single substrate structure for each enzyme. Another important difference, detailed below, concerns the treatment of inhibitor atoms that extend out of the active site and far into solution. The algorithm works as follows.

A cubic lattice with 0.2 Å spacing is superimposed on the binding site of the enzyme with bound substrate, and each grid point  $ijk$  within the van der Waals volume, using commonly accepted van der Waals radii (17), of any substrate atom other than hydrogen is

**Table 1:** Structures of substrates and ligands used for calculations

Substrate or ligand	PDB	Species/variant of receptor	RMSD <sup>a</sup>
<b>Abl kinase</b>			
<i>ADP</i>	<i>2g2i</i>	<i>Homo sapiens</i>	–
Imatinib	1opj	<i>Mus musculus</i>	1.08
Dasatinib	2gqg	<i>Homo sapiens</i>	0.80
PD180970	2hzi	<i>Homo sapiens</i>	1.05
VX-680	2f4j	<i>Homo sapiens</i>	0.78
<b>Chitinase</b>			
(NAG) <sub>5</sub>	<i>1e6n</i>	<i>Serratia marcescens</i>	–
Argadin	1w9u	<i>Aspergillus fumigatus</i>	1.41
Argifin	1w9v	<i>Aspergillus fumigatus</i>	1.43
Pentoxifylline	2a3c	<i>Aspergillus fumigatus</i>	1.41
<b>Thymidylate synthase</b>			
<i>Methylenetetrahydrofolate</i>	<i>1tsn</i>	<i>Escherichia coli</i>	–
BW1843U89	1tlc	<i>Escherichia coli</i>	0.44
Raltitrexed	2kce	<i>Escherichia coli</i>	0.32
<b>DHFR</b>			
<i>Dihydrofolate</i>	<i>1qzf</i>	<i>Cryptosporidium hominis</i>	–
WR99210	1j3i	<i>Plasmodium falciparum</i>	1.24
Pyrimethamine	1j3j	<i>Plasmodium falciparum</i> , mutant	1.17
Pyrimethamine	2bl9	<i>Plasmodium vivax</i>	1.16
Deschloropyrimethamine	2blb	<i>Plasmodium vivax</i>	1.16
<b>Neuraminidase</b>			
<i>Sialic acid</i>	<i>1mwe</i>	<i>A/Tern/Australia/G70C/75 (H1N9)</i>	–
Zanamivir	2cml	English duck subtype N6	0.39
G20	2qwi	<i>A/Tern/Australia/G70C/75 (H1N9)</i>	0.22
G28	2qwj	<i>A/Tern/Australia/G70C/75 (H1N9)</i>	0.09
Oseltamavir	2qwk	<i>A/Tern/Australia/G70C/75 (H1N9)</i>	0.11
Peramivir	117f	<i>A/Tern/Australia/G70C/75 (H1N9)</i>	0.12
Neu5Ac2en	1f8b	<i>A/Tern/Australia/G70C/75 (H1N9)</i>	0.09
4AM	1f8c	<i>A/Tern/Australia/G70C/75 (H1N9)</i>	0.08

Rows with PDB entries used for substrate envelope generation are italicized. Long (chemical) ligand names were replaced by codes used in the PDB file. <sup>a</sup>C $\alpha$  atom RMSD between the aligned substrate and ligand containing structures reported by SHEBA (18).

assigned a value of  $S_{ijk} = 1$ . All other grid points are assigned a value of  $S_{ijk} = 0$ . (The present software also allows fractional values between 0 and 1 as an indication of the percentage of substrate molecules lying on each grid point to handle cases, such as HIV protease, in which multiple substrate-bound structures are available.) The structure of the inhibitor-bound complex of interest is aligned with the substrate-bound complex using structural alignment program SHEBA (B. Lee, National Cancer Institute, Bethesda, MD) (18), and an analogous, overlapping cubic lattice with values  $I_{ijk}$  is computed for the inhibitor. The value of  $V_{out}$  can then be computed as the number of grid points  $ijk$  with  $I_{ijk} = 1$  and  $S_{ijk} = 0$ , multiplied by the volume of one grid cell,  $0.008 \text{ \AA}^3$ . Similarly, the volume of the inhibitor inside the substrate envelope,  $V_{in}$ , can be

computed from the number of inhibitor grid points with  $I_{ijk} = S_{ijk} = 1$ .

Inhibitor atoms that protrude far outside of the protein and into solution are not likely to be affected by mutations and thus, arguably, should not contribute to  $V_{out}$ . This issue is addressed by neglecting lattice points from the inhibitor grid that lie more than 4 Å from the nearest protein atom (see also ' $V_{out}$  correlates with overall mutation sensitivity of an inhibitor'). This threshold can cause part of the van der Waals volume of a ligand within a large binding cavity also to be excluded. This should not pose a problem, because these atoms presumably contribute little to the interaction with the protein.

Crystallographic water molecules are ignored in the present calculations. However, when crystallographic water that bridges the substrate and enzyme is thought to be critical to substrate binding, one may expect that mutations near the water molecule will affect substrate binding. In such cases, it may be useful to include the bound water as part of the substrate when defining the substrate envelope. If, on the contrary, a displaced water molecule is not thought to be essential for substrate binding, it likely can be ignored in the present approach.

Section ' $V_{out,loc}$  probes the local environment of the substrate envelope' analyzes the neuraminidase and DHFR systems, for which only a few mutation data are available. In these cases, values of  $V_{out,loc}$  were computed by furthermore neglecting lattice points from the inhibitor grid that lie more than 4 Å (unless specified otherwise) from any atom of a residue in the mutation set.

The 'Supporting Information' provides the FORTRAN source code for generating the substrate envelope grid, calculating  $V_{out}$  and  $V_{out,loc}$ , and converting the substrate envelope grid into a DX grid format, viewable with molecular graphics programs.

## Results

### $V_{out}$ correlates with overall mutation sensitivity of an inhibitor

The proposed correlation between  $V_{out}$  and the average sensitivity to mutation is best evaluated for a system with well-investigated mutant resistance profiles for multiple inhibitors, such as HIV protease. Figure 1 examines this correlation for the 5 inhibitors and 11 mutants with data taken from a previous study by Chellapan *et al.* (8). Good correlation is observed for the largest mutation set, ANAM-11, whereas a relatively low correlation is observed for L10I/L90M. Encouragingly, the *overall* sensitivity of an inhibitor to mutation, captured by the average of  $s_i$  over all mutants  $i$  (see 'Concepts and approach'), shows a smooth, monotonic increase with  $V_{out}$ , as shown by the thick line in Figure 1.

Similarly, Figure 2 plots average sensitivity to mutation against  $V_{out}$  for the other enzymes studied here; the plot for HIV protease, drawn from Figure 1, is included for comparison. The number of mutated residues is highest for the top graphs and falls for the lower graphs. It is therefore expected that any correlation that is

**Table 2:** Mutation set data sources used in this paper

Ligand	Data type	Mutation sets used in calculations <sup>a</sup>	Enzyme variant
Abl kinase Imatinib, dasatinib, PD180970, VX-680 (34)	$K_d$	Q252H, Y253F, E255K, T315I, T315N, M351T, F359V, H396P	Human Abl1 kinase
Chitinase Argadin, argifin (23), pentoxifylline (35)	$K_d$	T138A, D175A, A217G, M243A, R301K, E322A	<i>Aspergillus fumigatus</i> ChiB1 chitinase
Thymidylate synthase BW1843U89, raltitrexed	$IC_{50}$	K47E, D49G, G52S (36), I108A, I108F, L221A, L221I, L221S, F225L, F225W, F225Y (37)	Human
Dihydrofolate reductase Pyrimethamine, WR99210 (38)	$K_i$	K1 CB1 (C59R/S108N), V1/S (N51I/C59R/S108N/I164L)	<i>Plasmodium falciparum</i>
Pyrimethamine, deschloropyrimethamine (39)	$K_i$	SP21 (S58R/S117N)	<i>Plasmodium vivax</i>
Neuraminidase Zanamivir, oseltamivir, G20, G28, Neu5Ac2en, 4AM (12), peramivir (40)	$IC_{50}$	R292K	A/Tern/Australia/G70C/75 (H1N9) influenza
Peramivir, oseltamivir, zanamivir (41)	$IC_{50}$	E119G, E119A, E119D, R292K, H274Y, R152K	Influenza subtype A/N2 Influenza subtype A/N1 Influenza subtype B

<sup>a</sup>Single-site mutants, except for DHFR, where simultaneous mutations are parenthesized.

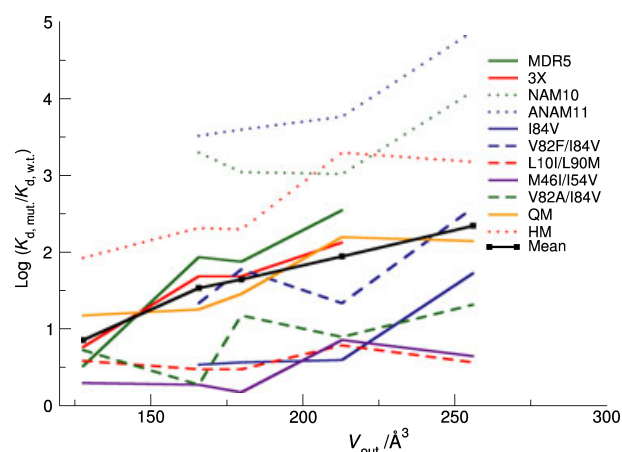


**Figure 1:** Correlation between the mutation sensitivity and  $V_{out}$  for five clinically approved HIV protease inhibitors and 11 mutation sets. From left to right, the points correspond to the following inhibitors: amprenavir, nelfinavir, indinavir, saquinavir, ritonavir. The thick line denotes the average of the resistances. The data are taken from Chellappan *et al.* (8). This and other plots in this paper were produced with Grace (<http://plasma-gate.weizmann.ac.il/Grace>).

observed will be clearest for the top graphs. This expectation is borne out by the data, as the top four graphs show a fairly high correlation between the mutation sensitivity and  $V_{out}$ , whereas the two bottom graphs do not. The latter will be analyzed below using the quantity  $V_{out,loc}$ . The slopes of the graphs, however, vary from system to system, even among the top graphs with their more extensive mutation sets. Despite the different slopes, these results show that  $V_{out}$  correlates with the inhibitors' sensitivity to target mutation for several different systems.

The three systems with the broadest data sets, HIV protease, Abl kinase, and chitinase, were further analyzed. Table 3 presents the correlation coefficients  $R$  of the average mutation sensitivity with  $V_{in}$ ,  $V_{out}$ , ratio  $V_{out}/V_{in}$ , several measures of inhibitor size [ $V_{tot}$ , molecular weight (M.W.),  $N_{heavy}$ ], and the Tanimoto coefficients (FP2, FP3) representing chemical similarity between substrate and ligands. Only  $V_{out}$  consistently correlates with the average mutation sensitivity for all the systems ( $R \geq 0.90$ ). Interestingly, although one might expect that measures of chemical similarity between substrate and ligand, such as the Tanimoto coefficients, would be useful in this context, in fact they do not perform as reliably as  $V_{out}$  (Table 3). This might reflect the fact that most of the ligands considered in Table 3 are very chemically different from the substrate: the average Tanimoto coefficient is only 0.38. It is also worth inquiring why the molecular size descriptors correlate with inhibitor sensitivity in only two of three cases, whereas  $V_{out}$  correlates well in all the three cases. When the inhibitors lie in essentially the same region as the substrate, as in HIV protease and chitinase, it is reasonable to expect that  $V_{out}$  will be roughly proportional to the size of the ligand. Indeed,  $V_{out}$  and M.W. are strongly correlated for HIV protease and chitinase ( $R = 0.97$  and  $0.99$ , respectively). However, if the inhibitor and substrate binding modes differ markedly, as in the large binding site of Abl kinase (Figure 3), the correlation between  $V_{out}$  and M.W. can be much lower (0.45 for Abl kinase), and the sensitivity of the inhibitors to mutations correlates with  $V_{out}$ , but not with simple measures of molecular size. These results are in accordance with the substrate envelope hypothesis.

The spatial overlap between inhibitor and substrate is quantified by  $V_{in}$ , and the ratio  $r = V_{in}/V_{out}$  may be expected to bear on the ability of the molecular size descriptors to correlate with overall mutation sensitivity, based upon the logic in the preceding paragraph. This suggestion is born out by the fact that  $r < 0.5$  for the Abl kinase inhibitors, and  $r > 0.8$  for chitinase and  $r > 1.2$  for HIV

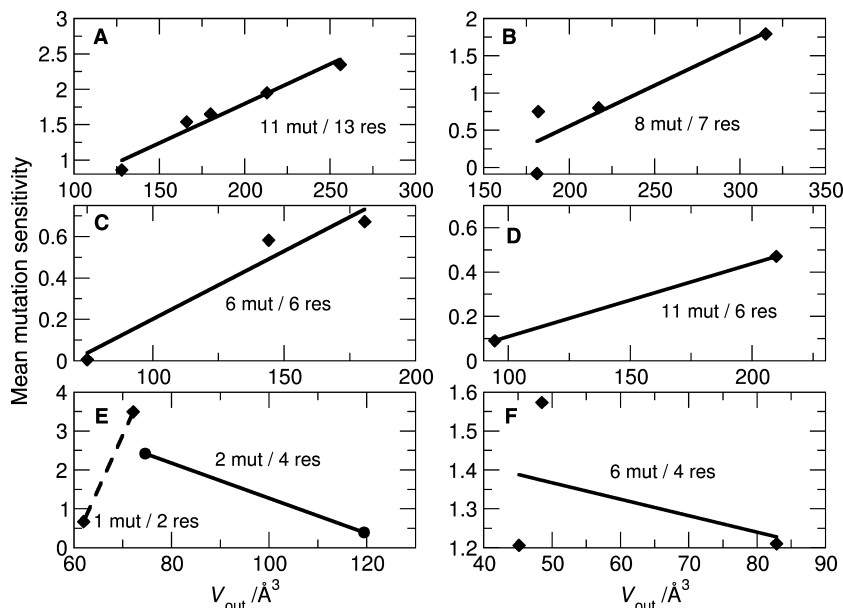


**Figure 2:** Average sensitivity to mutation of enzyme inhibitors versus volume outside the substrate envelope,  $V_{out}$ , for six systems: (A) HIV protease [amprenavir, nelfinavir, indinavir, saquinavir, ritonavir; data from Chellappan *et al.* (8)]. (B) Abl kinase (VX-680, PD-180970, dasatinib, imatinib). (C) Chitinase (pentoxifylline, argadin, argifin). (D) Thymidylate synthase (raltitrexed, BW1843U89). (E) Solid line: *Plasmodium falciparum* DHFR (pyrimethamine, WR99210); dashed line: *Plasmodium vivax* DHFR (deschloropyrimethamine, pyrimethamine). (F) neuraminidase (zanamivir, oseltamivir, peramivir). (Inhibitors are listed in order of increasing  $V_{out}$ .) Each panel lists the number of mutant enzymes over which the average sensitivities are computed, and the number of residues involved in these mutations. Neuraminidase inhibitors G20, G28, Neu5Ac2en, and 4AM (Table 2) are omitted from panel (F), because they have affinity data for only one mutant, R292K; this mutant is therefore considered separately.

**Table 3:** Correlation  $R$  between the average mutation resistance and volume outside of substrate envelope  $V_{out}$ , volume inside of substrate envelope  $V_{in}$ , ratio  $V_{out}/V_{in}$ , total molecular volume (heavy atoms)  $V_{tot}$ , molecular weight (M.W.), the number of non-hydrogen atoms ( $N_{heavy}$ ), and Tanimoto coefficients representing chemical similarity between substrate and ligand, for receptors with  $\geq 6$  mutated residues and  $\geq 3$  data points

Receptor	$V_{out}$	$V_{in}$	$V_{out}/V_{in}$	$V_{tot}$	M.W.	$N_{heavy}$	FP2 <sup>a</sup>	FP3 <sup>a</sup>
Abl kinase	0.90	-0.68	0.87	0.46	0.45	0.55	-0.18	0.18
Chitinase	0.97	0.51	0.62	0.99	0.99	0.99	0.98	0.99
HIV protease	0.98	0.81	0.95	0.98	0.94	0.97	0.5 <sup>b</sup>	0.55 <sup>b</sup>

Systems with two data points are not included because of the trivial fit.

<sup>a</sup>Tanimoto coefficients (number of bits in substrate/number of bits in ligand) were calculated using Daylight type fingerprints (FP2) and hexadecimal type fingerprints (FP3) between substrate and ligands.

<sup>b</sup>The average Tanimoto coefficients between individual ligands and six substrates (9) were used to generate data.

protease. In summary, although simple measures of size of the inhibitor may correlate with its sensitivity to mutation for some receptors, only  $V_{out}$  is expected to be a more broadly applicable guide to the design of robust inhibitors.

The present results are reasonably robust with respect to the cutoff distance used in calculating  $V_{out}$  (see 'Calculation of inhibitor volumes outside substrate envelope'). For example, using 3, 4, and 5 Å

cutoffs for Abl kinase yields correlations  $R = 0.89, 0.90,$  and  $0.81,$  respectively, whereas chitinase yields the same correlation ( $R = 0.97$ ) for all three cutoffs.

### Analysis of individual enzyme systems

#### Abl kinase

The values of  $V_{out}$  for four inhibitors of Abl tyrosine kinase, an important anti-cancer target (19), correlate well with their mutation sensitivity averaged over eight imatinib-resistant mutants, as evident from Figure 2B and Table 3. The molecular graphics in Figure 3 provide insight into the spatial relationships in this system. None of the inhibitors conform well to the shape of the substrate, and imatinib, in particular extends into a completely different region of the protein. As a consequence, only 62 Å<sup>3</sup> of its total volume of 405 Å<sup>3</sup> lie within the substrate envelope. The other three inhibitors are smaller and fit the substrate envelope better (Figure 3), although still not especially well: their total volumes range from 312 to 366 Å<sup>3</sup>, and their volumes within the substrate envelope range from 67 to 84 Å<sup>3</sup>. A recent report on the emergence of dasatinib-resistant mutations, V299L, T315A, and F317I that were not observed for imatinib previously (20), supports the observed lack of fit of dasatinib to the substrate envelope, and its consequent sensitivity to Abl kinase mutations. The large values of  $V_{out}$  for other inhibitors, although they are smaller than imatinib, suggest that new mutations could lead to resistance to the non-imatinib inhibitors.

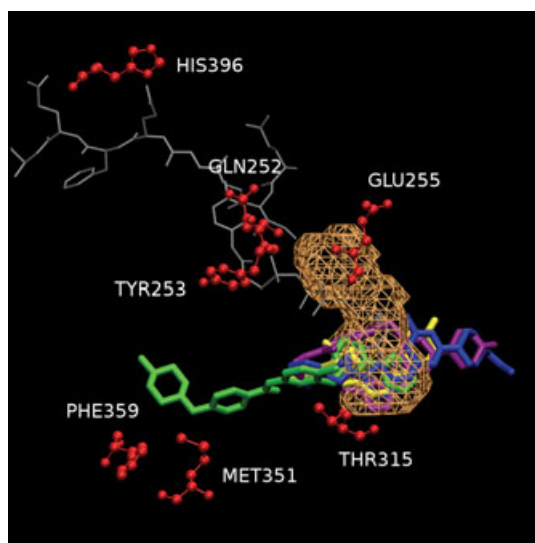


**Figure 3:** Abl kinase substrate envelope (orange) with superimposed inhibitors VX-680 (purple), PD-180970 (yellow), dasatinib (blue), and imatinib (green). Superposed ADP-peptide substrate conjugate (PDB entry 2g1t) is shown in gray. The inhibitors are represented as licorice sticks for clarity, but one should bear in mind that for substrate envelope calculations, the van der Waals radii were used. Mutated residues are depicted as red balls-and-sticks. Molecular graphics in this and other figures was produced using VMD (University of Illinois, Urbana-Champaign, IL) program (42).

Whether these four inhibitors would fit the substrate envelope better if one considered the substrate to be a protein tyrosine instead of the ADP substrate needs also to be considered. Superposition of a crystal structure of Abl kinase with a bound ADP-peptide conjugate (gray sticks in Figure 3) shows that the peptide moiety extends away from the bound inhibitors. Indeed,  $V_{out}$  computed for the investigated ligands using substrate envelope based upon ADP-peptide conjugate yields the same results as using ADP only.

It should be noted that Abl kinase can adopt both active and inactive conformations (21). While the calculations presented in the paper were performed using an active form of the kinase, we also computed values of  $V_{out}$  volumes using substrates bound to inactive (PDB ID: 2g2f) and Src-like inactive (2g1t) conformations of Abl kinase (21). The correlation of the  $V_{out}$  versus  $s$  results are essentially the same ( $R$  differs by 0.01) for the three investigated conformations.

### Chitinase

Chitinases belong to the glycohydrolase family of enzymes and are responsible for the degradation of chitin into  $\beta(1,4)$ -*N*-acetyl-D-glucosamine monomers (22). Inhibitors of chitinases have chemotherapeutic potential against pathogenic fungi, insects, malaria transmission, and human asthma (23). The values of  $V_{out}$  for 3 inhibitors solved with a family 18 chitinase are found here to correlate well with their sensitivity to mutation, averaged over 6 mutants, which emerged in organisms exposed to 2 of the inhibitors considered here, argifin and argadin (23) (Figure 2C and Table 3).

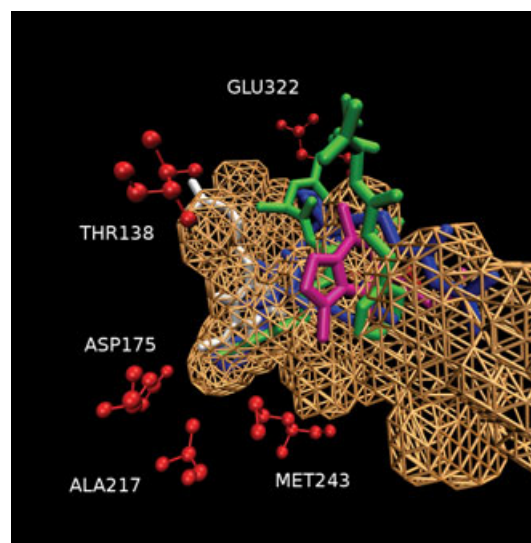


**Figure 4:** Chitinase substrate envelope (orange) with superimposed inhibitors pentoxifylline (white and purple), argadin (blue), and argifin (green). Argifin has the largest  $V_{out}$ , followed by argadin. Out of two pentoxifylline molecules in the binding site, the molecule drawn in white sticks has a smaller  $V_{out}$ .

The substrate in the present analysis is an *N*-acetylglucosamine pentamer, which occupies a narrow and deep groove in the enzyme spanning subsites  $-2$  to  $+3$  (24). Argifin and argadin are large, cyclic pentapeptides that overlap with part of the substrate, occupying subsites between  $-1$  and  $+2$  (23), and somewhat extending out of the binding cavity into solution, especially argifin (not illustrated here). This extension outside the binding site was one of the main motivations for employing a ligand-protein distance cutoff in the calculation of  $V_{out}$  (see 'Methods').

Pentoxifylline, the third inhibitor considered here, is considerably smaller than argifin and argadin, and crystallography shows two molecules of pentoxifylline in distinct locations of the active site (Figure 4). It is not known which location is more stable and hence more relevant enzymatically, although binding energy estimates (not detailed here) with the CHARMM (25) and DREIDING (26) force fields suggest that the first molecule (residue 1434 in the PDB file) binds more strongly than the second molecule (residue 1435), perhaps because the former occupies a deeper binding site inside the protein. Pentoxifylline, in the conformation of residue 1434 (white in Figure 4), fits the substrate envelope much better ( $V_{out} = 75 \text{ \AA}^3$ ) than the other residue 1435 (purple in Figure 4;  $V_{out} = 141 \text{ \AA}^3$ ). According to the substrate envelope hypothesis, conformation 1434 should be the one less affected by mutation and hence should be the preferred mode of binding to the mutants. Therefore, this conformation was the chief focus in the present study.

The enzymatic assay used to study this system provided quantitative data only for chitinase mutants that still bind the inhibitors fairly strongly. As a consequence, no data are available for highly resistant mutants, and the average resistance values in Figure 2C and Table 3 accordingly are relatively small. Interestingly, the Y245F

chitinase mutant, which for the same reason is absent from Figure 2C and Table 3, abrogates binding to argifin within the sensitivity limit of the method (23) but binds argadin detectably. This observation is consistent with the smaller  $V_{out}$  for argadin relative to argifin.

The structure with bound substrate corresponds to *Aspergillus fumigatus* chitinase, but the crystal structures with the three inhibitors correspond to the chitinase of the bacterium *Serratia marcescens*. The sequence identity of the two chitinases is only 27%, but the structural match is good: the root mean square deviation (RMSD) between the  $C\alpha$  coordinates of the two chitinases is 1.4 Å for all three inhibitor-bound structures. The match is even better inside the binding site. For example, residues that neighbor argifin in *A. fumigatus* chitinase have 71% identity with those in *Serratia marcescens*, and the RMSDs of argifin and argadin bound to *Serratia marcescens* chitinase (27), relative to *A. fumigatus* chitinase, are only 1.02 and 1.03 Å, respectively. These similarities support the significance of the present substrate envelope analysis.

### Thymidylate synthase

Human TS is the target of a number of existing and developmental cancer drugs (28), and has been the subject of extensive studies. For the present study, we identified two TS inhibitors, raltitrexed and BW1843U89, for which there are crystal structures bound to TS as well as resistance data for 11 TS mutants involving 6 sequence locations. Raltitrexed ( $V_{out} = 85 \text{ \AA}^3$ ) fits the substrate envelope better than BW1843U89 ( $V_{out} = 188 \text{ \AA}^3$ ) (Figure 5). This is consistent with the substrate envelope hypothesis, because it retains affinity for the mutants of TS better than BW1843U89 does (Figure 1D).

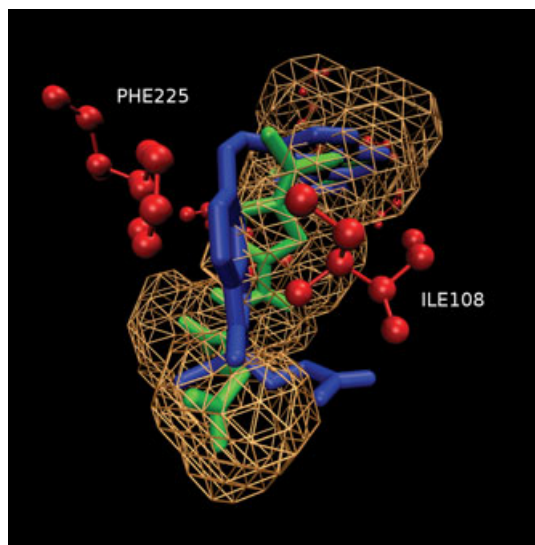


**Figure 5:** Thymidylate synthase substrate envelope (orange) with superimposed inhibitors BW1843U89 (blue) and raltitrexed (green). Only residues I108 and F225 whose mutations most strongly affect binding of these inhibitors are labeled. The larger sensitivity of BW1843U89 to the mutations is in agreement with the larger  $V_{out}$ .

Mutations of residues Ile 108 and Phe 225 have the strongest effect upon the binding of these inhibitors, and they, along with Leu 221, are also the residues that lie closest to the bound inhibitors, especially BW1843U89 (Figure 5).

The mutational affinity data considered here are based upon human TS, whereas the structural data are for *Escherichia coli* TS, because the requisite inhibitor structures were not available for the human enzyme. The structural data are considered relevant, however, because the two enzymes have overall 0.77 Å  $C\alpha$  RMSD with 97% of structurally matched residues. Furthermore, the gap between the values of  $V_{out}$  for the two inhibitors is substantial and cannot be accounted for by a structural mismatch between the two enzymes.

### Dihydrofolate reductase and neuraminidase

Dihydrofolate reductase is a target for anticancer (29), antibacterial (30) and antiprotozoal (31) treatments, whereas neuraminidase is one of the main therapeutic targets in the treatment of influenza (32). Here, the substrate envelope hypothesis is analyzed for two inhibitors and two mutants, involving four residues, of *Plasmodium falciparum* DHFR (Figure 2E, solid line); two inhibitors and one mutant, involving two residues, of *Plasmodium vivax* DHFR (Figure 2E, dashed line); and three inhibitors and six mutants, involving four residues, of neuraminidase (Figure 2F). The data summarized in Figure 2E and F do not show an overall correlation between an inhibitor's  $V_{out}$  and its sensitivity to mutation. This lack of correlation may result in part from the fact that the values of  $V_{out}$  for the inhibitors of DHFR and neuraminidase studied here cover relatively small ranges: compare the horizontal axes of Figure 2A–D with those of Figure 2E and F. Furthermore, the loss of correlation on moving to these two systems from the ones represented in Figure 2A–D is consistent with our expectation that the correlation would weaken as the number of residues probed by mutations falls (see ' $V_{out}$  correlates with overall mutation sensitivity of an inhibitor'): few mutated residues means more parts of the binding site where an inhibitor can project outside the substrate envelope without penalty.

### $V_{out,loc}$ probes the local environment of the substrate envelope

This subsection examines in more detail those systems for which  $V_{out}$  was not found to correlate well with an inhibitor's sensitivity to mutation; these are the same systems for which we have only a few mutation data, as noted above. In particular, we explore the idea that the sensitivity of an inhibitor to mutation correlates with the volume of the inhibitor outside the substrate envelope and close to the specific residues that are mutated,  $V_{out,loc}$ . The value of  $V_{out}$  is closely related to the sum of  $V_{out,loc}$  across multiple mutations. Therefore, if we find a correlation between the sensitivity to an individual mutation and  $V_{out,loc}$ , we can expect that a good correlation would be obtained between  $V_{out}$  and overall mutation sensitivity if we had a larger set of mutations that more completely probed the region around each inhibitor. Thus, the study of  $V_{out,loc}$  bears on the utility of  $V_{out}$  as a predictor of mutation sensitivity.

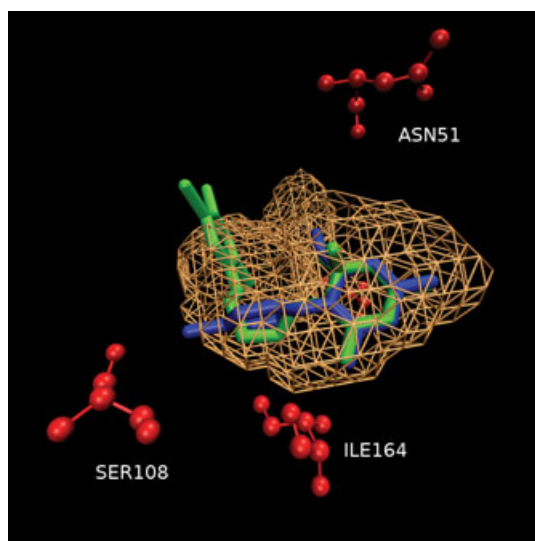


**Figure 6:** *Plasmodium falciparum* DHFR substrate envelope (orange) with superimposed inhibitors pyrimethamine (blue), WR99210 (green). Residue Cys59 is hidden behind the substrate envelope.

### Dihydrofolate reductase

We focus first on *P. falciparum* DHFR (Figure 2E, solid line), for which the inhibitor with the larger value of  $V_{out}$ , WR99210, is less sensitive to the studied mutations than the inhibitor with the smaller value of  $V_{out}$ , pyrimethamine. The part of WR99210 which extends outside the substrate envelope (Figure 6) remains far from the four residues affected by the mutations considered here. Pyrimethamine, on the contrary, does not extend as far outside the substrate envelope, but its extension is close to one of the mutated residues, Ser 108. These observations rationalize the observation that pyrimethamine is more sensitive than WR99210 to the mutations studied here, although its value of  $V_{out}$  is smaller. This idea is quantified by calculation of  $V_{out,loc}$ , which limits attention to places where an inhibitor extends outside the substrate envelope and also is close to a mutated residue. Figure 7 shows that this quantity does, in fact, correlate with the sensitivity of pyrimethamine and WR99210 to the mutations considered here.

In the case of *P. vivax* DHFR (Figure 2E, dashed line), the inhibitor's sensitivity to mutation increases with  $V_{out}$ , for these mutations. The

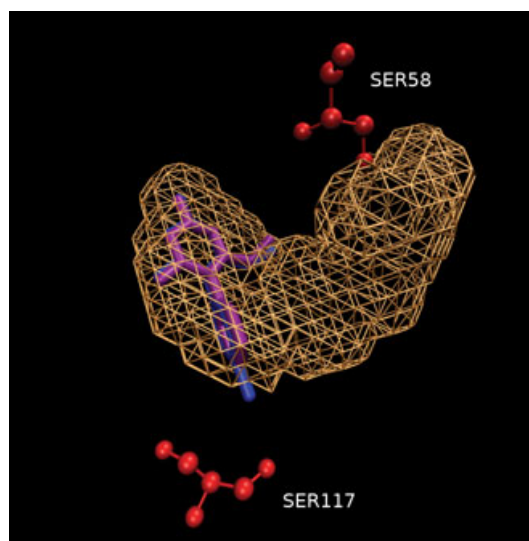


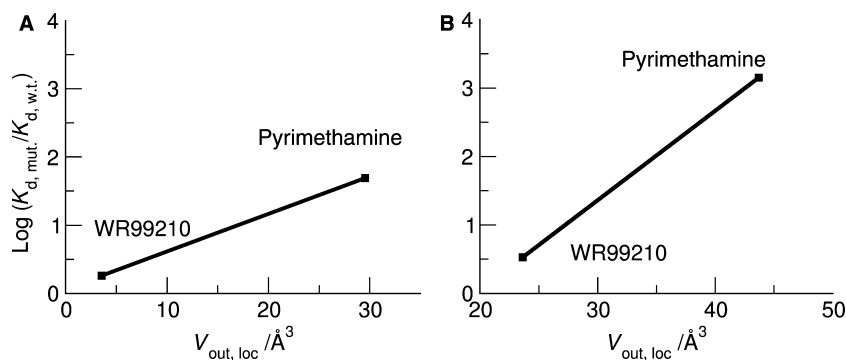
**Figure 8:** *Plasmodium vivax* DHFR substrate envelope (orange) with superimposed inhibitors pyrimethamine (blue) and deschloropyrimethamine (purple).

location where pyrimethamine (Figure 8) extends outside the substrate envelope is near one of the mutated residues, Ser 117. Deschloropyrimethamine fits the substrate envelope better there, and thus has a lower value of  $V_{out}$  and less sensitivity to mutation.

### Neuraminidase

Strains of the influenza virus show resistance to some of the neuraminidase inhibitors (33). Varghese *et al.* (12) noted a qualitative correlation between the degree of resistance of the R292K mutant and the degree of structural dissimilarity of the inhibitor to the transition-state analog. Here, similarly,  $V_{out}$  and  $V_{out,loc}$  are used to quantify the dissimilarity between substrate and inhibitors. Plots of  $V_{out}$  and  $V_{out,loc}$  against mutation sensitivity are compared (Figure 9) for six single-point mutations. Note that mutation sensitivity data for R292K are available for seven inhibitors, whereas the other five mutations (E199G, E119A, E119D, R152K, H274Y) have data for three inhibitors; for this reason, Figure 2F also contains three data points. Figure 10 shows that all the neuraminidase inhibitors analyzed here have shapes closely resembling the substrate; accordingly, their  $V_{out}$  and

**Figure 7:** Mutation sensitivity as a function of local  $V_{out}$  for *Plasmodium falciparum* DHFR: (A) mutation set K1 CB1, and (B) mutation set V1/S.



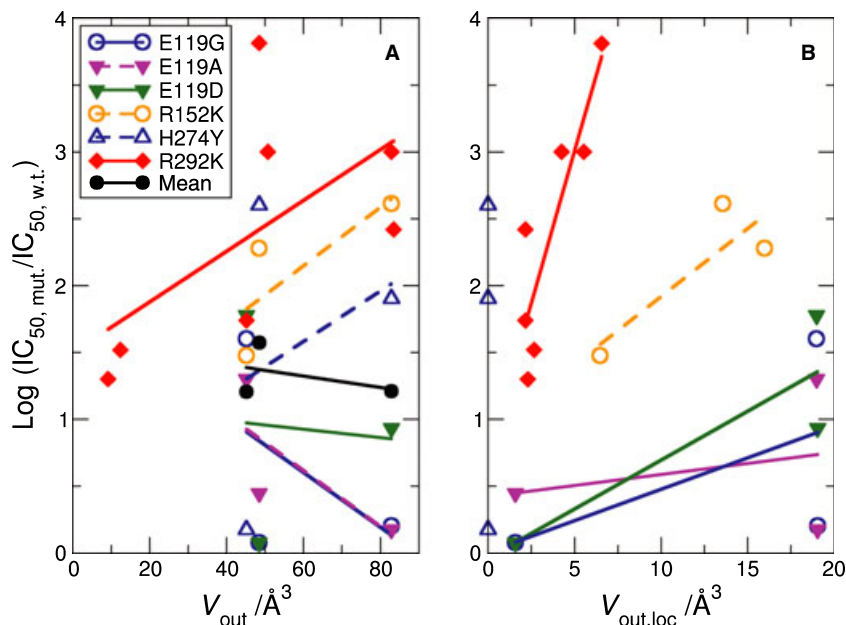


**Figure 9:** Mutation sensitivity against total (A) and local (B) volumes outside substrate envelope plotted for several neuraminidase mutations. The black points and line (corresponding to the average for three inhibitors) in (A) corresponds to the graph in Figure 2F. The  $V_{\text{out,loc}} = 0$  for H274Y mutation in (B), because His274 is situated beyond the used 4 Å cutoff from the inhibitors. To keep the graphs less busy, the names of compounds were not annotated.

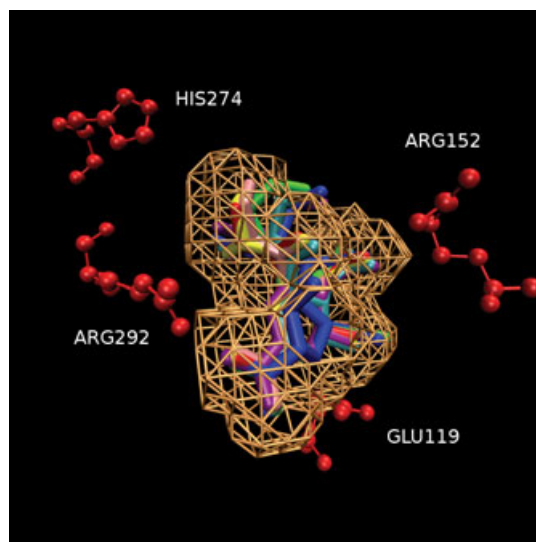


**Figure 10:** Neuraminidase substrate envelope (orange) with superimposed inhibitors 4AM (yellow), G20 (green), G28 (cyan), Neu5Ac2en (red), oseltamivir (purple), peramivir (blue), zanamivir (pink).

$V_{\text{out,loc}}$  values are relatively small, as evident from Figure 9B. Table 4 shows, not surprisingly, that  $V_{\text{out}}$  correlates poorly with the individual mutation sensitivities  $s$  of the inhibitors, with a mean correlation coefficient  $R = 0.06$ . However,  $V_{\text{out,loc}}$  exhibits a much better correlation with sensitivity (Figure 9B and column 2 of Table 4):  $R = 0.69$ . When the distance cutoff used in calculating  $V_{\text{out,loc}}$  is changed from 4 to 3 or 5 Å, the mean correlation for  $V_{\text{out,loc}}$  becomes 0.56 and 0.62, respectively. We therefore used the same 4 Å cutoff for the  $V_{\text{out,loc}}$  calculations as in the  $V_{\text{out}}$  calculations. However, the 4 Å cutoff failed to include H274Y mutation into the  $V_{\text{out,loc}}$  analysis (Figure 9), as van

**Table 4:** Correlation  $R$  between the mutation sensitivity against  $V_{\text{out}}$  and  $V_{\text{out,loc}}$  of neuraminidase inhibitors used in this study

Mutation	Data points	$V_{\text{out}}$	$V_{\text{out,loc}}$
E119G	3	-0.51	0.56
E119A	3	-0.74	0.28
E119D	3	-0.08	0.87
R152K	3	0.78	0.86
H274Y	3	0.31	n.a. <sup>a</sup>
R292K	7	0.61	0.89

<sup>a</sup>The ligand atoms are beyond default 4 Å cutoff from the His 274 residue.

der Waals spheres of all ligand atoms are beyond the 4 Å from His 274 residue.

The correlations observed here are consistent with the intuitive notion that a larger value of  $V_{\text{out,loc}}$  means a stronger interaction between the ligand and the mutated residue, and hence greater sensitivity to the mutation. On the contrary, the degree to which affinity is lost upon mutation of a given residue necessarily depends upon the details of the mutation (e.g., E199G, E119A or E119D); as  $V_{\text{out,loc}}$  is insensitive to these chemical details, it cannot be expected to provide precise predictions.

The comparatively extensive data for R292K were examined in more detail. The correlation coefficient,  $R$ , between  $V_{\text{out,loc}}$  and mutation sensitivity is 0.89, significantly higher than  $R = 0.61$  for  $V_{\text{out}}$ . In addition, the inhibitor that is most sensitive to the mutation, oseltamivir, is also the inhibitor with the largest value of  $V_{\text{out,loc}}$ : the van der Waals volume of oseltamivir extends beyond the substrate envelope near R292 (purple wireframe in Figure 11). On the contrary, the plot of sensitivity versus  $V_{\text{out,loc}}$  for R292K (Figure 9B) shows significant scatter. This may result in part from the small range of  $V_{\text{out,loc}}$  for the inhibitors for which R292K sensitivity data

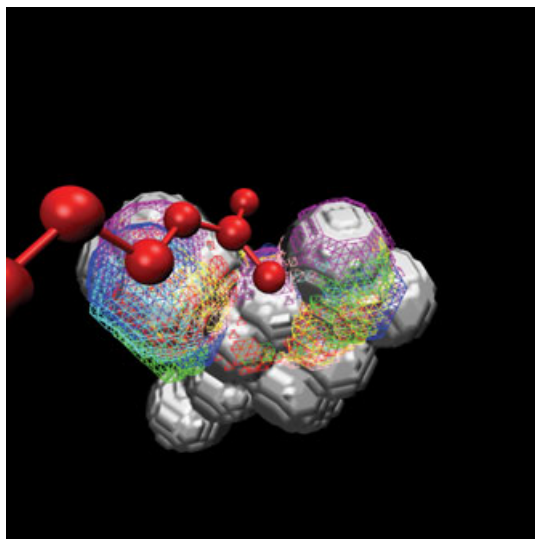


**Figure 11:** Visualization of volumes  $V_{out,loc}$  of neuraminidase inhibitors and off the substrate envelope (silver) in the neighborhood of Arg292 (represented by red balls-and-sticks): 4AM (yellow), G20 (green), G28 (cyan), Neu5Ac2en (red), oseltamivir (purple), peramivir (blue), zanamivir (pink).

are available. In addition, the range of mutation sensitivity is quite high, extending from 16- to 540-fold losses in affinity for the four inhibitors. The large range of sensitivities, despite a small range of  $V_{out,loc}$ , means that additional factors contribute significantly to the sensitivity of these inhibitors.

While we showed that  $V_{out,loc}$  can be a useful quantity, which could help our understanding of a sensitivity of a ligand toward a particular mutation, other factors may need to be included into a more comprehensive analysis, such as the chemical nature of the part of the ligand extending outside of the substrate envelope, shape and chemical moiety change invoked by the mutation, ligand flexibility and protein conformational changes upon binding and/or mutation. Because this paper introduces a simple shape-based descriptors of  $V_{out,loc}$  (and  $V_{out}$ ), extended analysis of these factors is beyond the scope of this paper.

## Discussion

This retrospective analysis further supports the hypothesis that enzyme inhibitors, which fit the substrate envelope tend to retain affinity in the face of clinically relevant mutations. By analyzing five additional enzyme systems, it generalizes prior studies that were limited to HIV protease (8,9). The present analysis also provides a deeper understanding of the underlying rationale for the substrate envelope hypothesis. In particular, we observe better correlation between  $V_{out}$  and the overall sensitivity of an inhibitor to a set of mutations when the set of mutations is extensive and thus probes ligand interactions with much of the binding pocket.

It is important to consider situations in which the substrate envelope concept might break down. One is the case where the receptor

adopts significantly different conformations in the context of bound substrate relative to bound inhibitor. This issue is addressed in part in the context of Abl kinase (see 'Abl kinase'), where the correlation between  $V_{out}$  and the mutation sensitivity of various inhibitors was found to be insensitive to the choice of receptor conformation. However, when more extensive conformational changes occur, it may become difficult to convincingly overlay the substrate envelope, computed from the substrate-bound conformation, on the inhibitor, bound to its very different protein conformation. In such cases, it might be possible to generalize the present approach by designing inhibitors which contact only those residues which contact the substrate, in relevant conformations of the enzyme. Alternatively, one could define the substrate envelope separately for each variant conformation of the enzyme, and total mutation resistance for the purpose of drug design could be considered as a combination of the  $V_{out}$  values for each conformation. The correlation between  $V_{out}$  and the sensitivity of an inhibitor to mutations could also break down because of flexibility of the inhibitor itself, as previously noted (10). In particular, an inhibitor that extends outside the substrate envelope may retain affinity to a mutant enzyme if the inhibitor adapts to the mutant by a change of conformation. Such adaptive inhibitors (5) offer another important avenue to robust inhibitors, which may be pursued in parallel with inhibitors that achieve robustness by remaining within the substrate envelope.

The functional dependence of  $V_{out}$  and mutation sensitivity is not necessarily linear, largely because  $V_{out}$  is insensitive to the specific chemistry of the inhibitor and mutations. Nonetheless, when a large mutation set is analyzed, a monotonic or close to monotonic increase is expected because sensitivity should not drop as  $V_{out}$  increases. This expectation is confirmed by the correlation between  $V_{out}$  and  $s$  for Abl kinase, chitinase, thymidylate synthase, and *P. vivax* DHFR, although the strength of the dependence of mutation sensitivity to  $V_{out}$  varies from one system to the next. However, for *P. falciparum* DHFR and neuraminidase, the mutation sensitivity drops as  $V_{out}$  increases. This observation was rationalized by the fact that the available mutations are few and thus do not probe all the interactions of the inhibitors with their binding pockets. However, the mutation sensitivity of these inhibitors correlates with the quantity  $V_{out,loc}$ , which measures the degree to which an inhibitor projects from the substrate envelope near known mutations. This observation strongly suggests that the sensitivity of inhibitors to mutation would indeed correlate with  $V_{out}$  if a larger mutation set were available.

The fit of an inhibitor or candidate inhibitor to the substrate envelope, as measured by the quantity  $V_{out}$ , represents a simple way to anticipate its robustness in the face of mutations both known and unknown, and the present study shows that this idea is applicable to many therapeutic targets. The software included in the 'Supporting Information' quickly provides the value of  $V_{out}$  (and  $V_{out,loc}$ ) for a bound ligand, and the  $V_{out}$  can then be used as a figure of merit along with the usual binding score. Although the quantity  $V_{out,loc}$  can be useful in analyzing known mutations,  $V_{out}$  should be more useful in the prospective design of new inhibitors. The use of such relatively simple parameters should help future novel inhibitors to retain affinity to the wide and unpredictable range of target mutations that can occur in a quickly evolving, highly mutable therapeutic enzyme target.

## Acknowledgments

We thank Fundação para a Ciência e a Tecnologia (Portugal) for Grant SFRH/BPD/41787/2007 attributed to V. Kairys and SFRH/BPD/30954/2006 attributed to V. Lather. This publication was made possible by the National Institute of General Medical Sciences (NIGMS) of the NIH Grants No. GM61300, GM62050 (to M. K. Gilson) and GM65347, GM66524 (to C. A. Schiffer). The contents of this publication are solely the responsibility of the authors and do not necessarily represent the official views of the NIGMS.

## References

- Soulsby E.J. (2005) Resistance to antimicrobials in humans and animals. *Br Med J*;331:1219–220.
- Dorman S.E., Chaisson R.E. (2007) From magic bullets back to the magic mountain: the rise of extensively drug-resistant tuberculosis. *Nat Med*;13:295–298.
- Hochhaus A., Erben P., Ernst T., Mueller M.C. (2007) Resistance to targeted therapy in chronic myelogenous leukemia. *Semin Hematol*;44:S15–S24.
- Longley D.B., Johnston P.G. (2005) Molecular mechanisms of drug resistance. *J Pathol*;205:275–292.
- Ohtaka H., Freire E. (2005) Adaptive inhibitors of the HIV-1 protease. *Prog Biophys Mol Biol*;88:193–208.
- King N.M., Prabu-Jeyabalan M., Nalivaika E.A., Schiffer C.A. (2004) Combating susceptibility to drug resistance: lessons from HIV-1 protease. *Chem Biol*;11:1333–1338.
- Hellen C.U.T., Kräusslich H.-G., Wimmer E. (1989) Proteolytic processing of polyproteins in the replication of RNA viruses. *Biochemistry*;28:9881–9890.
- Chellappan S., Kairys V., Fernandes M.X., Schiffer C., Gilson M.K. (2007) Evaluation of the substrate envelope hypothesis for inhibitors of HIV-1 protease. *Proteins*;68:561–567.
- Chellappan S., Reddy G.S.K.K., Ali A., Nalam M.N.L., Anjum S.G., Cao H., Kairys V., Fernandes M.X., Altman M.D., Tidor B., Rana T.M., Schiffer C.A., Gilson M.K. (2007) Design of mutation-resistant HIV protease inhibitors with the substrate envelope hypothesis. *Chem Biol Drug Des*;69:298–313.
- Altman M.D., Ali A., Reddy G.S., Nalam M.N., Anjum S.G., Cao H., Chellappan S., Kairys V., Fernandes M.X., Gilson M.K., Schiffer C.A., Rana T.M., Tidor B. (2008) HIV-1 protease inhibitors from inverse design in the substrate envelope exhibit subnanomolar binding to drug-resistant variants. *J Am Chem Soc*;130:6099–6113.
- Schiffer C.A. (2008) Combating drug resistance – identifying resilient molecular targets and robust drugs. In: Stroud R.M., Finer-Moore J., editors. *Computational and structural approaches to drug discovery*. The Royal Society of Chemistry, Cambridge, UK; p. 127–133.
- Varghese J.N., Smith P.W., Sollis S.L., Blick T.J., Sahasrabudhe A., McKimm-Breschkin J.L., Colman P.M. (1998) Drug design against a shifting target: a structural basis for resistance to inhibitors in a variant of influenza virus neuraminidase. *Structure*;6:735–746.
- Colman P.M. (2002) Neuraminidase inhibitors as antivirals. *Vaccine*;20(Suppl 2):S55–S58.
- Colman P.M. (2005) Zanamivir: an influenza virus neuraminidase inhibitor. *Expert Rev Anti Infect Ther*;3:191–199.
- Berman H.M., Westbrook J., Feng Z., Gilliland G., Bhat T.N., Weissig H. *et al.* (2000) The Protein Data Bank. *Nucl Acids Res*;28:235–242.
- Liu T., Lin Y., Wen X., Jorissen R.N., Gilson M.K. (2007) Binding-DB: a web-accessible database of experimentally determined protein-ligand binding affinities. *Nucleic Acids Res*;35:D198–D201.
- Bondi A. (1964) van der Waals volumes and radii. *J Phys Chem*;68:441–451.
- Jung J., Lee B. (2000) Protein structure alignment using environmental profiles. *Protein Eng*;13:535–543.
- Ren R. (2005) Mechanisms of BCR-ABL in the pathogenesis of chronic myelogenous leukaemia. *Nat Rev Cancer*;5:172–183.
- Shah N.P., Skaggs B.J., Branford S., Hughes T.P., Nicoll J.M., Paquette R.L., Sawyers C.L. (2007) Sequential ABL kinase inhibitor therapy selects for compound drug-resistant BCR-ABL mutations with altered oncogenic potency. *J Clin Invest*;117:2562–2569.
- Levinson N.M., Kuchment O., Shen K., Young M.A., Koldobskiy M., Karplus M., Cole P.A., Kuriyan J. (2006) A Src-like inactive conformation in the abl tyrosine kinase domain. *PLoS Biol*;4:e144.
- Hurtado-Guerrero R., van Aalten D.M.F. (2007) Structure of *Saccharomyces cerevisiae* chitinase 1 and screening-based discovery of potent inhibitors. *Chem Biol*;14:589–599.
- Rao F.V., Houston D.R., Boot R.G., Aerts J.M.F.G., Hodgkinson M., Adams D.J., Shiomi K., Ōmura S., van Aalten D.M.F. (2005) Specificity and affinity of natural product cyclopentapeptide inhibitors against *A. fumigatus*, human, and bacterial chitinases. *Chem Biol*;12:65–76.
- van Aalten D.M.F., Komander D., Synstad B., Gåseidnes S, Peter M.G., Eijsink V.G.H. (2001) Structural insights into the catalytic mechanism of a family 18 exo-chitinase. *Proc Natl Acad Sci USA*;98:8979–8984.
- MacKerell A.D. Jr, Bashford D., Bellott M., Dunbrack R.L., Evanseck J.D., Field M.J., Fischer S. *et al.* (1998) All-Atom Empirical Potential for Molecular Modeling and Dynamics Studies of Proteins. *J Phys Chem B*;102:3586–3616.
- Mayo S.L., Olafson B.D., Goddard W.A. (1990) DREIDING: a generic force field for molecular simulations. *J Phys Chem*;94:8897–8909.
- Houston D.R., Shiomi K., Arai N., Ōmura S., Peter M.G., Turberg A., Synstad B., Eijsink V.G.H., van Aalten D.M.F. (2002) High-resolution structures of a chitinase complexed with natural product cyclopentapeptide inhibitors: mimicry of carbohydrate substrate. *Proc Natl Acad Sci U S A*;99:9127–9132.
- Costi M.P., Ferrari S., Venturelli A., Calò S., Tondi D., Barlocco D. (2005) Thymidylate synthase structure, function and implication in drug discovery. *Curr Med Chem*;12:2241–2258.
- McGuire J.J. (2003) Anticancer antifolates: current status and future directions. *Curr Pharm Des*;9:2593–2613.
- Hawser S., Lociuro S., Islam K. (2006) Dihydrofolate reductase inhibitors as antibacterial agents. *Biochem Pharmacol*;71:941–948.

31. Anderson A.C. (2005) Targeting DHFR in parasitic protozoa. *Drug Discov Today*;10:121–128.
32. Moscona A. (2005) Neuraminidase inhibitors for influenza. *N Engl J Med*;353:1363–1373.
33. Reece P.A. (2007) Neuraminidase inhibitor resistance in influenza viruses. *J Med Virol*;79:1577–1586.
34. Carter T.A., Wodicka L.M., Shah N.P., Velasco A.M., Fabian M.A., Treiber D.K., Milanov Z.V. *et al.* (2005) Inhibition of drug-resistant mutants of ABL, KIT, and EGF receptor kinases. *Proc Natl Acad Sci U S A*;102:11011–11016.
35. Rao F.V., Andersen O.A., Vora K.A., DeMartino J.A., van Aalten D.M.F. (2005) Methylxanthine drugs are chitinase inhibitors: investigation of inhibition and binding modes. *Chem Biol*;12:973–980.
36. Tong Y., Liu-Chen X., Ercikan-Abali E.A., Capioux G.M., Zhao S.C., Banerjee D., Bertino J.R. (1998) Isolation and characterization of thymitaq (AG337) and 5-fluoro-2-deoxyuridylate-resistant mutants of human thymidylate synthase from ethyl methane-sulfonate-exposed human sarcoma HT1080 cells. *J Biol Chem*;273:11611–11618.
37. Tong Y., Liu-Chen X., Ercikan-Abali E.A., Zhao S.C., Banerjee D., Maley F., Bertino J.R. (1998) Probing the folate-binding site of human thymidylate synthase by site-directed mutagenesis. Generation of mutants that confer resistance to raltitrexed, Thymitaq, and BW1843U89. *J Biol Chem*;273:31209–31214.
38. Yuvaniyama J., Chitnumsub P., Kamchonwongpaisan S., Vanichananukul J., Sirawaraporn W., Taylor P., Walkinshaw M.D., Yuthavong Y. (2003) Insights into antifolate resistance from malarial DHFR-TS structures. *Nat Struct Biol*;10:357–365.
39. Kongsaree P., Khongsuk P., Leartsakulpanich U., Chitnumsub P., Tarnchompoo B., Walkinshaw M.D., Yuthavong Y. (2005) Crystal structure of dihydrofolate reductase from *Plasmodium vivax*: pyrimethamine displacement linked with mutation-induced resistance. *Proc Natl Acad Sci U S A*;102:13046–13051.
40. Smith B.J., McKimm-Breshkin J.L., McDonald M., Fernley R.T., Varghese J.N., Colman P.M. (2002) Structural studies of the resistance of influenza virus neuraminidase to inhibitors. *J Med Chem*;45:2207–2212.
41. Gubareva L.V., Webster R.G., Hayden F.G. (2001) Comparison of the activities of zanamivir, oseltamivir, and RWJ-270201 against clinical isolates of influenza virus and neuraminidase inhibitor-resistant variants. *Antimicrob Agents Chemother*;45:3403–3408.
42. Humphrey W., Dalke A., Schulten K. (1996) VMD: visual molecular dynamics. *J Mol Graph*;14:33–38.

### Supporting Information

Additional Supporting Information may be found in the online version of this article:

1. Mutation sensitivities which were used in the paper, by the inhibitor and mutation (Table S1);
2. FORTRAN programs: (a) to generate the substrate envelope grid; (b) to convert it into a grid format viewable with several molecular graphics programs; and (c) to compute  $V_{out}$  and  $V_{out,loc}$ .

Please note: Wiley-Blackwell is not responsible for the content or functionality of any supporting materials supplied by the authors. Any queries (other than missing material) should be directed to the corresponding author for the article.